

## Effects of Suction and Blowing on Flow Separation in a Symmetric Sudden Expanded Channel

G. C. Layek<sup>1</sup>, C. Midya<sup>2</sup>, S. Mukhopadhyay<sup>3</sup>

<sup>1</sup>Department of Mathematics, The University of Burdwan, Burdwan, W.B., India  
math\_gclayek@buruniv.ac.in; goralayek@yahoo.com

<sup>2</sup>Department of Mathematics, S. S. College, Jiaganj, Murshidabad, W.B., India

<sup>3</sup>Department of Mathematics, M. U. C. Women's College, Burdwan, W.B., India

**Received:** 15.07.2007    **Revised:** 04.06.2008    **Published online:** 28.11.2008

**Abstract.** A numerical simulation has been carried out to study the laminar flow in a symmetric sudden expanded channel subjected to a uniform blowing/suction speed placed at the lower and upper porous step walls. The governing equations for viscous flow have been solved using finite-difference techniques in pressure-velocity formulation. The results obtained here have been compared with the available experimental and numerical results of similar problems. It is noted that the recirculating region formed near the step walls diminishes in its length for increasing values of blowing speed applied at the porous step walls. For a suitable blowing speed, the recirculation zone disappears completely. The critical Reynolds number for the flow bifurcation (i.e. flow asymmetry) is obtained and it increases with the increase of the blowing speed. The critical Reynolds number for symmetry breaking of the flow decreases with the increasing values of suction speeds. The primary and the secondary recirculating regions formed near the channel walls are controlled using blowing.

**Keywords:** sudden expansion, porous step walls, staggered grid.

### 1 Introduction

Laminar separated flows and the control of flow separation belong to one of the fundamental classes of flows which have attracted substantial attention in fluid mechanics over the years. Two-dimensional laminar flow of an incompressible Newtonian fluid in a symmetric sudden expanded channel has been studied by several investigators. Experimental and numerical studies of Durst et al. [1], Cherdron et al. [2], Sobey and Drazin [3], Fearn et al. [4], and Durst et al. [5] investigated the sudden expansion channel flows with moderate expansion ratio. When the Reynolds number  $Re$  is relatively low, the flow is symmetric and the recirculating regions at the two channel walls are also symmetric. With the increase of Reynolds number, the flow remains two-dimensional but asymmetry of the flow sets in. Additional recirculation zones appear along the channel walls for further higher values of  $Re$ . Recently, Chiang et al. [6] reported the sidewall effects in

a symmetric sudden expansion flow via 2-D and 3-D simulations. Hawa and Rusak [7] used an asymptotic analysis to investigate the resulting change in the bifurcation diagram and stability in a slightly asymmetric channel with a sudden expansion. Using asymptotic analysis, Hawa and Rusak [8] demonstrated that when the Reynolds number is smaller than a critical value,  $Re_c$ , the symmetric states have an asymptotically stable mode of disturbance. However, when  $Re > Re_c$ , the symmetric states are unstable to this mode of asymmetric disturbance. The asymmetry of the flow depends on the Reynolds number of the flow, the expansion ratio and also on the aspect ratio (Durst et al. [5]).

Separation control (with active or passive methods) is of immense importance to the performance of air, land or sea vehicles, turbomachines, diffusers, and a variety of other technologically important systems involving fluid flow (see Gad-el-Hak and Bushnell [9]). There are several methods which have been developed for the purpose of artificial control of the boundary layer behaviour e.g. near-wall fluid suction and blowing, cooling and heating, surface modifications in the form of hump and dip, flow streaming by favourable pressure gradient. According to the physical concept of the boundary layer, it is possible to delay or even prevent separation by removing the decelerated fluid particles caused by the adverse pressure gradient in the region where separation is likely to develop. The much explored method of preventing separation is suction because it is relatively easy to impose the various strengths of surface mass flow to perturb the laminar flow separation. The effect of suction consists in the removal of directed fluid particles from the boundary layer before they are given a chance to cause separation. On the other hand, the wall shear stress and hence friction drag is reduced by blowing. That is why blowing may be useful in controlling the flow separation in a system involving fluid flow. Wall blowing and suction have been encountered in many engineering flow problems such as turbine-blade cooling, transition delay and prevention of separation. Comprehensive summaries of research in the area of boundary layer control by suction or injection in the flow of a viscous fluid are to be found in Lachmann et al. [10] and Chang et al. [11]. Recently, Kaiktsis and Monkewitz [12] investigated the effects of wall suction applied at the step wall on flow separation in backward-facing step flow.

In the present paper, we explore the effects of suction and blowing speeds placed at the porous step walls on flow separation and symmetry-breaking bifurcation in a two-dimensional sudden expanded channel. Finite-difference approximations of the governing equations of motion in the primitive variable formulation are employed. The recirculation regions near the step walls can be influenced by a suitable imposition of blowing and suction speed at the porous step walls. Wall shear stress distribution which is a function of suction or blowing speed has been calculated and presented graphically. The pattern of streamlines and the vorticity contours have been drawn and analysed physically. The critical Reynolds number for which the symmetry breaking bifurcation of the flow occurred is obtained.

## 2 Governing equations

We consider the two-dimensional flow of an incompressible viscous fluid of constant density  $\rho$ , in a two-dimensional symmetric sudden expanded channel. Let  $(x^*, y^*)$  be

the Cartesian coordinates of any point in the flow domain, where the  $x^*$ -axis is along the bottom plate of the outlet channel and  $y^*$  is the normal to both the plates. Let  $u^*, v^*$  be the velocity components along the  $x^*$  and  $y^*$  directions respectively,  $p^*$  the pressure and  $U$  the maximum velocity at the inlet section of the channel. A physical sketch of the problem is given in Fig. 1. The height of the inlet channel is  $h$ . Let  $x_1^*, x_2^*$  denote the upper wall and lower wall reattachment lengths respectively. The channel height is taken as  $s^*$ .

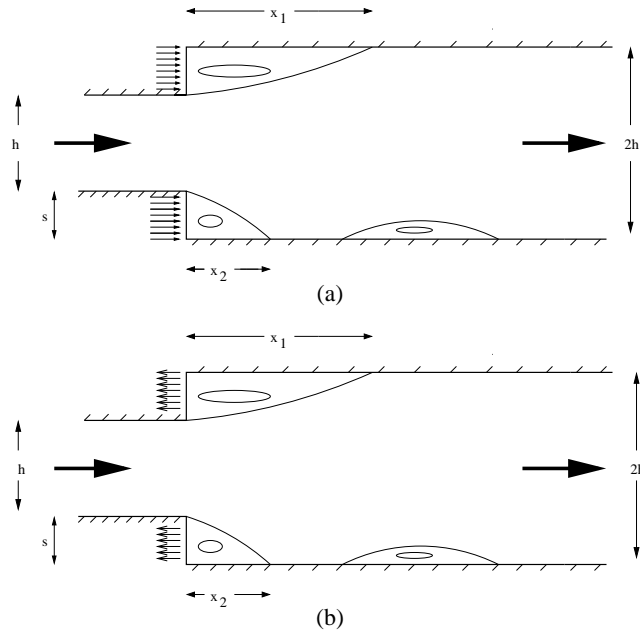


Fig. 1. Schematic diagram of the flow configuration, in the presence of (a) blowing; (b) suction at the step walls.

Introducing the following dimensionless variables

$$\begin{aligned} t &= t^*U/h, & x &= x^*/h, & y &= y^*/h, & u &= u^*/U, & v &= v^*/U, \\ p &= p^*/\rho U^2, & x_r &= x_r^*/h, \end{aligned} \quad (1)$$

the Navier-Stokes equations for motion are written as

$$\frac{\partial u}{\partial x} + \frac{\partial v}{\partial y} = 0, \quad (2)$$

$$\frac{\partial u}{\partial t} + \frac{\partial u^2}{\partial x} + \frac{\partial uv}{\partial y} = -\frac{\partial p}{\partial x} + \frac{1}{Re} \left( \frac{\partial^2 u}{\partial x^2} + \frac{\partial^2 u}{\partial y^2} \right), \quad (3)$$

$$\frac{\partial v}{\partial t} + \frac{\partial uv}{\partial x} + \frac{\partial v^2}{\partial y} = -\frac{\partial p}{\partial y} + \frac{1}{Re} \left( \frac{\partial^2 v}{\partial x^2} + \frac{\partial^2 v}{\partial y^2} \right), \quad (4)$$

where  $Re = Uh/\nu$  is the Reynolds number. The non-dimensional step height is taken as  $s$  where  $s = s^*/h$ . The channel expansion ratio is taken as 1 : 2. The non-dimensional length of the inlet channel is taken as 4.

### 3 Boundary conditions

The streamwise and transverse velocity components should be zero at the rigid walls (no-slip condition) except at the porous step walls where a blowing or suction of fluid with speed  $u_b$  or  $u_s$  is imposed. The suction or injection speed is kept small in comparison with the main stream velocity  $U$ . At the inlet section of the channel the flow is assumed to be fully developed i.e., Poiseuille flow.

The downstream length measured from the step is sufficiently long (45 non-dimensional units), so that the reattachment length is independent of the length of the computational domain. The boundary condition at the outlet cross-section of the channel was taken as that of a fully developed flow, i.e.  $\frac{\partial u}{\partial x} = \frac{\partial v}{\partial x} = 0$ .

### 4 Numerical methods

The governing equations (2), (3) and (4) along with the initial and boundary conditions are solved by a finite difference method. Control volume-based finite-difference discretization of the above equations is carried out on a staggered grid, popularly known as MAC (Marker and Cell) proposed by Harlow and Welch [13]. In this type of grid alignment, the velocities and the pressure are evaluated at different locations of the control volume.

The time derivative terms are differenced according to the first-order accurate two-level forward time-differencing formula. The convective terms in the momentum equations are differenced with a hybrid scheme consisting of the central differencing and the second-order upwinding in order to reduce or eliminate “false diffusion”. The diffusive terms are differenced by a second-order accurate three-point central difference formula. The source terms are centrally differenced, keeping the position of the respective fluxes at the centres of the control volumes. Thus, in finite-difference form, with  $t = n\Delta t$ ,  $x = i\Delta x$ ,  $y = j\Delta y$  and  $p(x, y, t) = p(i\Delta x, j\Delta y, n\Delta t) = p_{i,j}^n$ , where the superscript  $n$  refers to the time direction,  $\Delta t$  is the time increment and  $\Delta x$ ,  $\Delta y$  are the length and width of the  $(i, j)$ -th control volume.  $(x_i, y_j)$  and  $(x_{i+\frac{1}{2}}, y_{i+\frac{1}{2}})$  are the co-ordinates of the cell centre and the right top corner of the cell, respectively.

The discretized form of the continuity equation at the  $(i, j)$  cell becomes

$$\frac{u_{i+\frac{1}{2},j}^n - u_{i-\frac{1}{2},j}^n}{\Delta x} + \frac{v_{i,j+\frac{1}{2}}^n - v_{i,j-\frac{1}{2}}^n}{\Delta y} = 0. \quad (5)$$

Considering the source, convective and diffusive terms at the  $n$ -th time level, the momentum equation in the  $x$ -direction given by equation (3) is put in the finite-difference form

$$\frac{u_{i+\frac{1}{2},j}^{n+1} - u_{i+\frac{1}{2},j}^n}{\Delta t} = \frac{p_{i,j}^n - p_{i+1,j}^n}{\Delta x} + \text{Ucd}_{i,j}^n, \quad (6)$$

where

$$\text{Ucd}_{i,j}^n = \frac{1}{Re} \text{Diff}u_{i,j}^n - \text{Con}u_{i,j}^n. \quad (7)$$

Here  $\text{Diff}u_{i,j}^n$  and  $\text{Con}u_{i,j}^n$  are the diffusive and convective terms of the  $u$ -momentum equation for the  $n$ -th time level at  $(i, j)$  cell. The diffusive terms are discretized centrally. A central difference formula is used for the mixed derivative  $\partial^2 u / \partial x \partial y$  in uniform grid sizes.

The same discretization techniques are employed for the  $v$ -momentum equation and the final form of discretized equation becomes

$$\frac{v_{i,j+\frac{1}{2}}^{n+1} - v_{i,j+\frac{1}{2}}^n}{\Delta t} = \frac{p_{i,j}^n - p_{i,j+1}^n}{\Delta y} + \text{Vcd}_{i,j}^n, \quad (8)$$

where

$$\text{Vcd}_{i,j}^n = \frac{1}{Re} \text{Diff}v_{i,j}^n - \text{Con}v_{i,j}^n. \quad (9)$$

Here  $\text{Diff}v_{i,j}^n$  and  $\text{Con}v_{i,j}^n$  are the finite-difference representation of diffusive and convective terms of the  $v$ -momentum equation for the  $n$ th time level at the cell  $(i, j)$ .

A Poisson equation for pressure is obtained by combining the discretized form of the momentum and continuity equations. The final form of the Poisson equation for pressure is

$$\begin{aligned} & 2(A + B)p_{i,j}^n - Ap_{i+1,j}^n - Ap_{i-1,j}^n - Bp_{i,j-1}^n - Bp_{i,j+1}^n \\ & = - \left[ \frac{\text{Div}_{i,j}^n}{\Delta t} + \frac{\text{Ucd}_{i,j}^n - \text{Ucd}_{i-1,j}^n}{\Delta x} + \frac{\text{Vcd}_{i,j}^n - \text{Vcd}_{i,j-1}^n}{\Delta y} \right]. \end{aligned} \quad (10)$$

Here  $\text{Div}_{i,j}^n$  is the finite-difference representation of the divergence of the velocity field at cell  $(i, j)$ . The expressions for  $A, B$  are presented below.

$$A = \frac{1}{(\Delta x)^2}, \quad B = \frac{1}{(\Delta y)^2}.$$

The advantage in using MAC cell is that the pressure boundary condition is not needed at the boundaries where the velocity vector is specified, because the domain boundaries are chosen to fall on velocity nodes. For the cells adjacent to the upper wall ( $y = 2$ ), we get from  $v$ -momentum equation

$$p_{i,j+1}^n = p_{i,j}^n + \Delta y \text{Vcd}_{i,j}^n. \quad (11)$$

Thus the Poisson equation for pressure for the cells adjacent to the upper wall ( $y = 2$ ) is

$$\begin{aligned} & (2A + B)p_{i,j}^n - Ap_{i+1,j}^n - Ap_{i-1,j}^n - Bp_{i,j-1}^n \\ & = - \left[ \frac{\text{Div}_{i,j}^n}{\Delta t} + \frac{\text{Ucd}_{i,j}^n - \text{Ucd}_{i-1,j}^n}{\Delta x} - \frac{\text{Vcd}_{i,j-1}^n}{\Delta y} \right], \end{aligned} \quad (12)$$

where  $p_{i,j}^n$  is the pressure located at the cell centre inside the flow domain.

The Poisson equation for pressure for the cells adjacent to the inlet channel boundary at  $x = 0$  can be expressed as

$$(A + 2B)p_{i,j}^n - Ap_{i+1,j}^n - Bp_{i,j-1}^n - Bp_{i,j+1}^n = - \left[ \frac{\text{Div}_{i,j}^n}{\Delta t} + \frac{\text{Ucd}_{i,j}^n}{\Delta x} + \frac{\text{Vcd}_{i,j}^n - \text{Vcd}_{i,j-1}^n}{\Delta y} \right], \quad (13)$$

where  $p_{i,j}^n$  is the pressure at the cell centre inside the flow domain.

Similarly, the Poisson equations for pressure for the cells adjacent to the step height wall, inlet channel lower wall and outlet channel lower wall and outlet boundary are obtained. The Poisson equation for pressure (equation (10)) is solved iteratively by successive over-relaxation (S.O.R.) method. The value of the over-relaxation parameter is taken here as 1.2.

In the correction stage, pressure and subsequently the velocities are corrected to get a more accurate velocity field in the sense that it will satisfy the continuity equation more accurately. This second stage begins with computing the divergence of the velocity field for each cell. If it is found to be greater than  $0.5 \times 10^{-6}$  at any cell in absolute sense, then the pressure is corrected for each cell in the flow field. The velocity components at the sides of the cell are then adjusted. The pressure correction formula is

$$p_{i,j}^n = p_{i,j}^* + \omega \Delta p_{i,j}, \quad (14)$$

where  $p_{i,j}^*$  is obtained after solving the Poisson equation,  $\omega$  ( $\omega \leq 0.5$ ) is an under-relaxation parameter and

$$\Delta p_{i,j} = - \frac{\text{Div}_{i,j}^*}{2\Delta t(A + B)}, \quad (15)$$

where  $\text{Div}_{i,j}^*$  is the value of the divergence of velocity field at the cell  $(i, j)$  obtained after solving the Poisson equation for pressure. The  $u$ -velocity correction formulae are:

$$u_{i+\frac{1}{2},j}^{n+1} = u_{i+\frac{1}{2},j}^* + \frac{\Delta t \Delta p_{i,j}}{\Delta x}, \quad (16)$$

$$u_{i-\frac{1}{2},j}^{n+1} = u_{i-\frac{1}{2},j}^* - \frac{\Delta t \Delta p_{i,j}}{\Delta x}, \quad (17)$$

where  $u_{i+\frac{1}{2},j}^*$ ,  $u_{i-\frac{1}{2},j}^*$  represent the updated velocity field obtained after solving the Poisson equation for pressure. Similarly, the  $v$ -velocity corrections could be obtained.

The Courant-Fredrichs-Lewy (CFL) condition and the condition which is related to the viscous effects, according to Hirt's stability criterion (that is, the momentum must not diffuse farther than one cell in one time step) were used to determine the time step  $\Delta t$  (see Hirt [14]). The final time step was less than the minimum determined by the above two conditions. A typical value of the time step for the present computation in the Reynolds number range 100 to 500 is 0.006. For higher Reynolds number flow, the time step (consistent with the above two conditions) had to be reduced further. The details can be found in Midya et al. [15].

## 5 Results and discussion

Grid independent tests have been performed for selecting the final grid-size of the present computation. The reattachment lengths on both the upper and the lower wall have been presented at Table 1 for different grid sizes when  $u_b = u_s = 0$  and  $Re = 300$ . The results are compared with the experimental results of Durst et al. [5] for the reattachment length at  $Re = 300$  and  $u_b = 0.0$  (at which lower and upper wall reattachment lengths are near about 5.39 and 17.1 respectively) and are found to agree well in case of lower grid sizes (i.e.  $\Delta x = \Delta y = 0.04$ ). Grid independent tests have also been performed for two cases, one for  $u_b = 0.05$  and another for  $u_s = 0.05$ . The primary separation lengths at the lower and upper walls for  $u_b = 0.05$  and  $u_s = 0.05$  have been shown in the Table 2 and Table 3 respectively. All the computations have been carried out in a Pentium IV machine with a speed 2.4 of GHz and 256 MB RAM.

Table 1. Reattachment lengths at the lower and upper walls for different grid sizes for  $Re = 300$  and  $u_b = 0.0$

grid	lower wall	upper wall
$0.04 \times 0.04$	5.373	16.963
$0.06 \times 0.06$	5.782	15.824
$0.08 \times 0.08$	6.100	15.737

Table 2. Primary separation lengths at the lower and upper wall for different grid sizes for  $Re = 300$  and  $u_b = 0.05$

grid	lower wall	upper wall
$0.04 \times 0.04$	3.28	6.71
$0.06 \times 0.06$	3.34	6.67
$0.08 \times 0.08$	3.39	6.56

Table 3. Primary separation lengths at the lower and upper wall for different grid sizes for  $Re = 300$  and  $u_s = 0.05$

grid	lower wall	upper wall
$0.04 \times 0.04$	2.22	8.13
$0.06 \times 0.06$	2.27	8.08
$0.08 \times 0.08$	3.31	8.02

The verification of the present numerical algorithm is performed against experimental and numerical results for the case of symmetric sudden expansion channel. The results obtained in this study have been compared with the experimental and numerical studies of Durst et al. [5] and are presented in Fig. 2. In this figure, we present recirculation zone lengths, normalized by step height  $s$  ( $s = 1/2$ ), versus Reynolds number,  $Re$ . The computational values obtained by using the present numerical scheme agree well with the numerical and experimental findings of Durst et al. [5]. The dependence of

the details of the flow on the dimensionless parameters, say, Reynolds number ( $Re$ ) and suction/blowing speed is investigated systematically in the following sections.

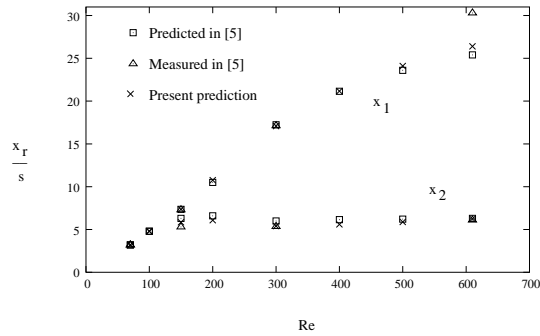


Fig. 2. Recirculation length,  $x_r$ , normalized by step height,  $s$ , versus Reynolds number  $Re$  for the comparison of experimental and numerical results.

### 5.1 Pattern of flow

First of all we present the figures which establishes the mirror image field in the flow. Fig. 3 depicts the pattern of streamlines reflecting mirror image view for  $u_s = 0, 0.05, 0.1$  and  $Re = 100$ . The recirculating region increases on both lower and upper walls equally when the suction velocity ( $u_s$ ) is 0.05. Its length further increases for  $u_s = 0.1$ .

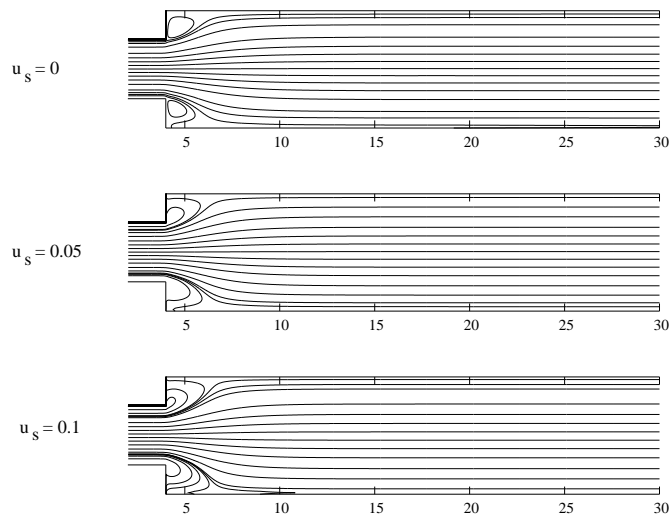


Fig. 3. Pattern of streamlines for different values of suction speeds for the Reynolds number  $Re = 100$  (the  $x$ - and  $y$ -scales are not the same).

Fig. 4 exhibits the vortex shedding of the flow pattern for different suction velocities ( $u_s = 0, 0.05, 0.1$ ) for the same Reynolds number. The same feature of vorticity field (mirror-image) is viewed.

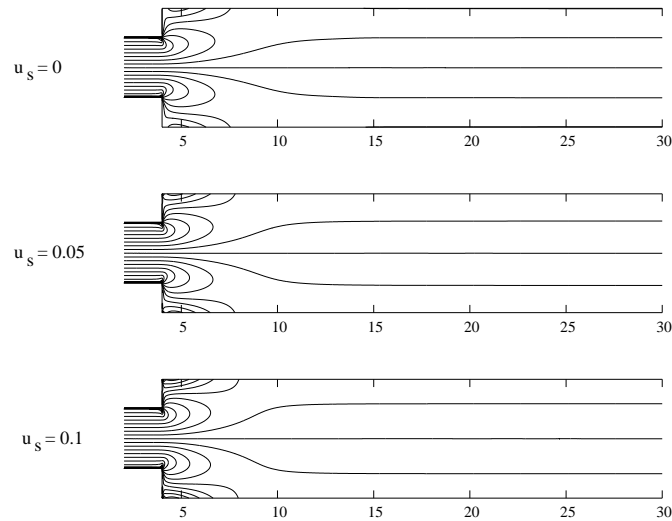


Fig. 4. Vorticity isocontours for different values of suction speeds for the Reynolds number  $Re = 100$  (the  $x$ - and  $y$ -scales are not the same).

We have also drawn curves of wall shear stresses (Figs. 5(a) and (b)) for both walls taking same values of suction speeds and Reynolds number. The same feature as cited above is retained in the distribution of wall stresses.

Fig. 6 presents the velocity distribution at the location of  $x = 5$  near the step wall (the inlet channel length has been taken as 4, i.e. upto  $x = 4$ ). It is clear that, when  $u_s = 0$ , the upper and the lower parts of the velocity curves have negative regions indicating the presence of recirculation zones in both the channel walls. The length of recirculation zone increases for the increased values of suction speeds. The flow field becomes asymmetric.

Fig. 7 shows the streamlines for  $u_b = 0, 0.05, 0.1$  for the Reynolds number 300. It is seen, however, that as  $u_b$  increases, the length of separation also gradually diminishes along the upper wall of the channel whereas increases gradually along the lower wall of the channel and the streamline pattern gradually becomes symmetric as  $u_b$  increases.

Isovorticity lines have some interesting features, and are shown in Fig. 8 at the Reynolds number 300. In the non-manipulated ( $u_b = 0$ ) flow, the centreline vorticity contour is curved which starts at the junction of inlet channel and outlet channel. This indicates the asymmetric nature of the flow. When  $u_b = 0.05$  is imposed, the contours become more symmetric than  $u_b = 0$  and centreline vorticity line also tends to a straight line. For  $u_b = 0.1$ , the centreline becomes nearly straight line and contours are almost symmetric about the centreline of the channel.

Figs. 9(a) and 9(b) represent non-dimensional shear stress distribution

( $[\tau_w = \tau / (\frac{1}{2}\rho U^2)]$ ) along the upper and lower outlet walls respectively for various values of the blowing at  $Re = 300$ . With the increase in blowing speeds, it is seen from Fig. 9 that the upper wall shear stresses decrease significantly near the upper step wall. For the

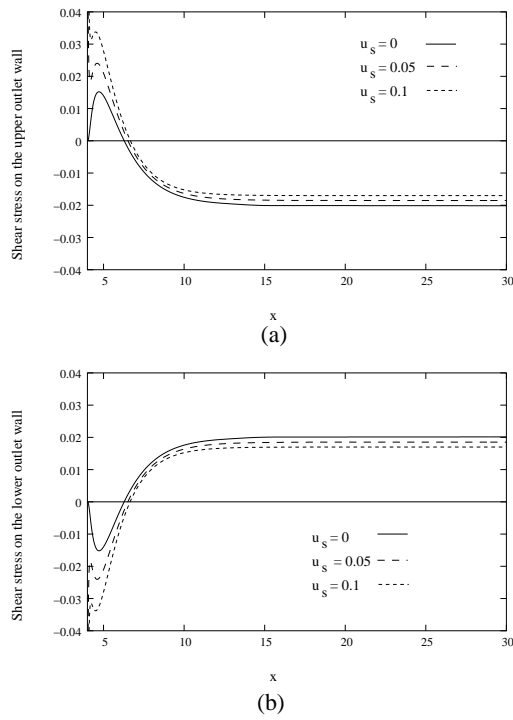


Fig. 5. Shear stress distribution: (a) along the upper outlet wall, for  $u_s = 0, 0.05, 0.1$  and  $Re = 100$ ; (b) along the lower outlet wall, for  $u_s = 0, 0.05, 0.1$  and  $Re = 100$ .

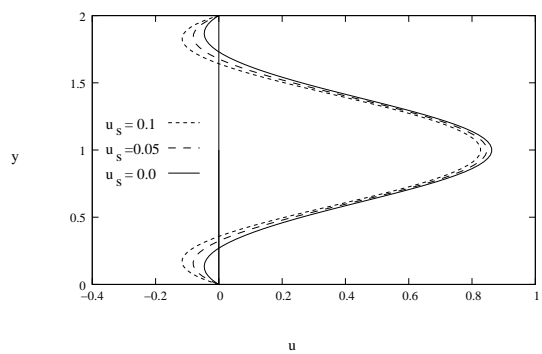


Fig. 6. Velocity profiles at a station  $x = 5$  for  $u_s = 0, 0.05, 0.1$  and  $Re = 100$ .

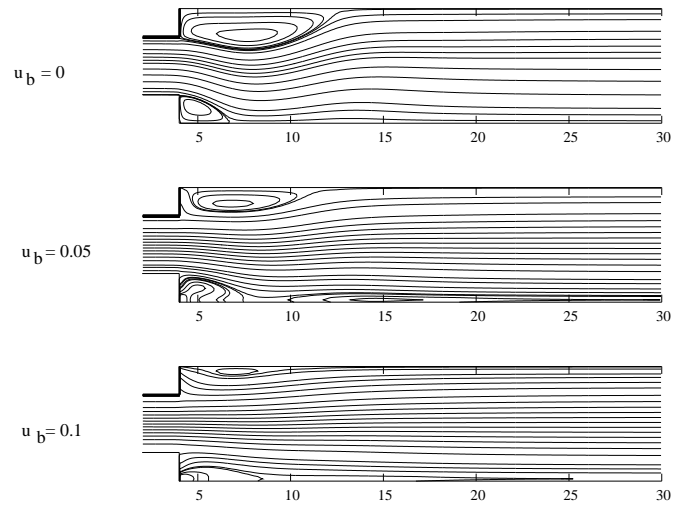


Fig. 7. Pattern of streamlines for different values of blowing speeds for the Reynolds number  $Re = 300$  (the  $x$ - and  $y$ -scales are not the same).

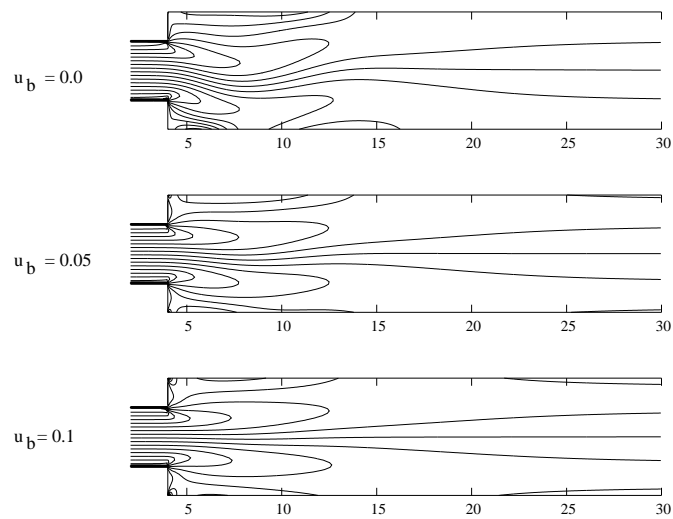


Fig. 8. Vorticity isocontours for different values of blowing speeds for the Reynolds number  $Re = 300$  (the  $x$ - and  $y$ -scales are not the same).

non-manipulated flow case, the graph for the wall shear stress shows that there is a big primary separation, near the upper step wall. With the application of small blowing speed, say  $u_b = 0.05$ , this large separation zone decreases in its size and for the blowing speed  $u_b = 0.1$ , the large separation region has been drastically decreased in length. Hence, blowing can be used as an alternative method for controlling separation. Due to the application of blowing at the porous step walls, the decelerated fluid particles are accelerated, resulting in the decrease of region of separation.

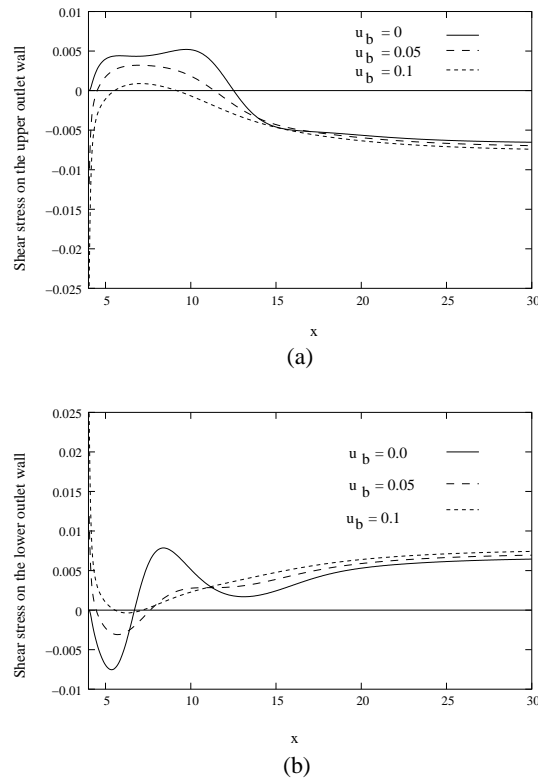


Fig. 9. Shear stress distribution: (a) along the upper outlet wall, for  $u_b = 0, 0.05, 0.1$  and  $Re = 300$ ; (b) along the lower outlet wall, for  $u_b = 0, 0.05, 0.1$  and  $Re = 300$ .

The velocity curve at the location of  $x = 5$  near the step wall (the inlet channel length has been taken as 4, i.e. upto  $x = 4$ ) is shown in the Fig. 10. The velocity curves have negative regions showing the recirculation zones in both the channel walls for  $u_b = 0$ . The separation zones on both the walls decrease its length for the application of blowing speed  $u_b = 0.05$ . The velocity curve for  $u_b = 0.1$  has no negative region which indicates the flow separation region is completely disappeared.

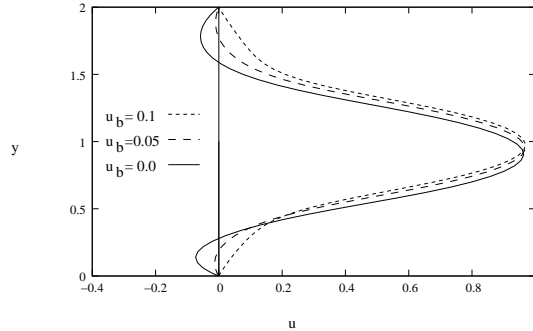


Fig. 10. Velocity profiles at a station  $x = 5$  for  $u_b = 0, 0.05, 0.1$  and  $Re = 300$ .

### 5.2 Asymmetric flow

Now, we measure asymmetry of the flow by the root mean square  $v$ -velocity ( $v_{rms}$ ) on the centreline of the channel. The  $v_{rms}$  is defined as

$$v_{rms} = \sqrt{\frac{v_{i+\frac{1}{2},j}^2 + v_{i+\frac{3}{2},j}^2 + v_{i+\frac{5}{2},j}^2 + \dots + v_{i+\frac{2n-1}{2},j}^2}{n}}$$

$j$  lies on the centreline of the channel,  $n$  is the total number of grid points in the axial direction. When  $v_{rms}$  is close to zero, the flow becomes symmetric. Fig. 11 depicts  $v_{rms}$  versus  $Re$  for various values of  $u_b$  and  $u_s$ . Obviously, the flow remains symmetric up to a specific Reynolds number depending upon the situation considered. It is to be noted that the critical Reynolds number denoted by  $Re_c$  is obtained close to 125 for  $u_b = u_s = 0$ . With further increase in Reynolds number, the asymmetry of the flow develops which turns up another strong recirculating region. Fig. 11 indicates that for blowing speed  $u_b = 0.05$  the flow field remains symmetric up to  $Re = 185$  approximately. The critical

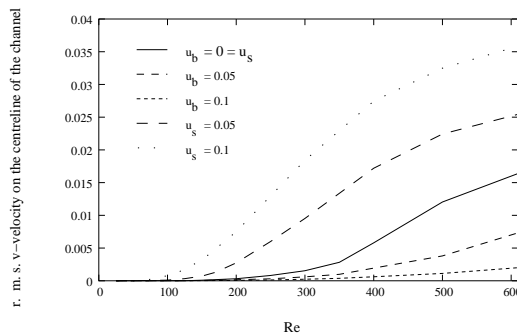


Fig. 11. Distribution of r.m.s.  $v$ -velocity on the channel centreline against  $Re$  for different values of blowing and suction speeds.

Reynolds number is near about 260 when the blowing speed is  $u_b = 0.1$ . On the contrary, if we impose suction velocity at the steps, the flow is found to be more unstable, and an early asymmetry occurs. When  $u_s = 0.05$ , the flow becomes asymmetric at a Reynolds number of 90 approximately and for suction speed  $u_s = 0.1$ , the critical value is found near about 75. Therefore, imposition of blowing at the step walls increases the flow's stability to asymmetric perturbations, and can also prevent separation. On the other hand, suction can be used as an asymmetry generator.

## 6 Conclusions

The structure of a two-dimensional flow in a channel with sudden expansion subject to blowing and suction at the porous step walls has been studied. The Navier-Stokes equations have been solved by a finite difference method using staggered grid. Asymmetric states appear when  $Re > Re_c$ . Shear stress distributions have been determined for different blowing and suction speeds. The critical Reynolds numbers for the flow asymmetry bifurcation have been obtained for various blowing and suction speeds. Based on the present results, the following observations can be made.

1. In the region of large recirculation zone, shear stress values decrease significantly at increasing blowing speed.
2. By the application of blowing, the separation point shifts towards downstream of the channel and the reattachment point towards the upstream direction of the channel.
3. Thus, blowing shrinks the large recirculation zone, and in the case of suction, the separating enhances.
4. The blowing through the channel wall makes the asymmetric nature of flow to the symmetric by diminishing the region of separation. On the other hand, the symmetric nature of flow becomes asymmetric by the application of suction from the porous channel wall and the region of separation enhances due to increasing suction speed.
5. The critical Reynolds number for flow symmetry bifurcation increases with the increase of blowing intensity.

## Acknowledgements

The authors would like to express their sincere gratitude to the referees for their constructive comments and suggestions which enable us to improve this paper in the present form. One of the author G. C. Layek acknowledges the financial support from CSIR project, New Delhi, India, sanction No. 25(0148)/06/EMR-II.

## References

1. F. Durst, A. Melling, J.H. Whitelaw, Low Reynolds number flow over a plane symmetrical sudden expansion, *J. Fluid Mech.*, **64**, pp. 111–128. 1974.

2. W. Cherdron, F. Durst, J. H. Whitelaw, Asymmetric flows and instabilities in symmetric ducts with sudden-expansion, *J. Fluid Mech.*, **84**, pp. 13–31 1978.
3. I. J. Sobey, P. G. Drazin, Bifurcation of two-dimensional channel flows, *J. Fluid Mech.*, **171**, pp. 256–287, 1986.
4. R. M. Fearn, T. Mullin, K. A. Cliffe, Nonlinear flow phenomena in a symmetric sudden expansion, *J. Fluid Mech.*, **211**, pp. 595–608, 1990.
5. F. Durst, J. C. Pereira, C. Tropea, The plane symmetric sudden-expansion flow at low Reynolds numbers, *J. Fluid Mech.*, **248**, pp. 567–581, 1993.
6. T. P. Chiang, T. W. H. Sheu, S. K. Wang, Sidewall effects on the structure of laminar flow over a plane-symmetric sudden expansion, *Comput. Fluids*, **29**(5), pp. 467–492, 2000.
7. T. Hawa, Z. Rusak, Viscous flow in a slightly asymmetric channel with a sudden expansion, *Phys. Fluids*, **12**(9), pp. 2257–2267, 2000.
8. T. Hawa, Z. Rusak, The dynamics of a laminar flow in a symmetric channel with a sudden expansion, *J. Fluid Mech.*, **436**, pp. 283–320, 2001.
9. M. Gad-el-Hak, D. M. Bushnell, Separation Control: Review, *Trans. ASME J. Fluids Eng.*, **113**, pp. 5–30, 1991.
10. *Boundary layer and flow control*, Vols. I, II, G. V. Lachmann (Ed.), Pergamon Press, London, 1961.
11. P. K. Chang, *Control of flow separation*, Hemisphere Publ. Corp. Washington, DC, 1976.
12. L. Kaiktsis, P. A. Monkewitz, Global destabilization of flow over a backward-facing step, *Phys. Fluids*, **15**(12), pp. 3647–3658, 2003.
13. F. H. Harlow, J. E. Welch, Numerical calculation of time dependent viscous incompressible flow of fluid with free surface, *Phys. Fluids*, **8**, pp. 2182–2189, 1965.
14. C. W. Hirt, Heuristic stability theory for finite-difference equations, *J. Comput. Phys.*, **2**, pp. 339–355, 1968.
15. C. Midya, G. C. Layek, A. S. Gupta, T. R. Mahapatra, Magnetohydrodynamic viscous flow separation in a channel with constrictions, *Trans. ASME J. Fluids Eng.*, **125**, pp. 952–962, 2003.